

# Supercapacitor Devices Based on Graphene Materials

Yan Wang,<sup>†</sup> Zhiqiang Shi,<sup>‡</sup> Yi Huang,<sup>†</sup> Yanfeng Ma,<sup>†</sup> Chengyang Wang,<sup>\*,‡</sup> Mingming Chen,<sup>‡</sup> and Yongsheng Chen<sup>\*,†</sup>

Key Laboratory of Functional Polymer Materials and Center for Nanoscale Science & Technology, Institute of Polymer Chemistry, College of Chemistry, Nankai University, Tianjin 300071, China, and Key Laboratory for Green Chemical Technology of State Education Ministry, School of Chemical Engineering and Technology, Tianjin University, Tianjin 300072, China

Received: March 12, 2009; Revised Manuscript Received: May 3, 2009

Graphene materials (GMs) as supercapacitor electrode materials have been investigated. GMs are prepared from graphene oxide sheets, and subsequently suffer a gas-based hydrazine reduction to restore the conducting carbon network. A maximum specific capacitance of 205 F/g with a measured power density of 10 kW/kg at energy density of 28.5 Wh/kg in an aqueous electrolyte solution has been obtained. Meanwhile, the supercapacitor devices exhibit excellent long cycle life along with ~90% specific capacitance retained after 1200 cycle tests. These remarkable results demonstrate the exciting commercial potential for high performance, environmentally friendly and low-cost electrical energy storage devices based on this new 2D graphene material.

## 1. Introduction

It is now essential that new, low-cost and environmentally friendly energy storage systems be found, in response to the needs of modern society and emerging ecological concerns.<sup>1</sup> Supercapacitors (also called electrochemical capacitors and ultracapacitors),<sup>2,3</sup> one of the energy storage systems, are able to store and deliver energy at relatively high rates (beyond those accessible with batteries) because the mechanism of energy storage is the simple charge-separation at the electrochemical interface between the electrode and the electrolyte.<sup>2,4</sup> One particular advantage for supercapacitors is that they have several orders of magnitude higher energy density than that of conventional dielectric capacitors.<sup>2</sup> Furthermore, the deficiencies of other power sources, such as batteries and fuel cells, could be complemented by supercapacitors, owing to their long cycle life and rapid charging and discharging at high power densities.<sup>5</sup> Since 1957, when the practical use of electrochemical capacitors, for the storage of electrical charge, was demonstrated and patented by General Electric,<sup>6</sup> supercapacitors have generated great interest for a wide and growing range of applications, including load cranes, forklifts, electric vehicles, electric utilities, factory power backup and so on.<sup>4,5,7</sup> So far, different materials, such as various carbon materials,<sup>2,8–15</sup> mixed metal oxides<sup>16–18</sup> and conducting polymers,<sup>19</sup> have been used as supercapacitor electrode materials. Particularly, carbon, in its various forms,<sup>2,8–15</sup> has been used as electrode materials of supercapacitors, aiming at high specific capacitance together with high power density. Although porous carbon materials have high specific surface area, the low conductivity of porous carbon materials is limiting its application in high power density supercapacitors.<sup>15</sup> Carbon nanotubes (CNTs), with excellent electrical conductivity and high surface areas, have been fabricated for supercapacitors since 1997.<sup>8,13,20,21</sup> However, CNT-based supercapacitors have not met the expected performance; one possible reason is probably due to the observed contact resistance between the electrode and current collector.<sup>15,22</sup> Hence, many studies have focused on the

morphology of the carbon materials to boost the performance of the capacitor,<sup>11,13,15,23–25</sup> such as growing CNTs directly on bulk metals to eliminate the contact resistance.<sup>12,15</sup> Graphene, with one-atom thick layer 2D structure,<sup>26,27</sup> is emerging as a unique morphology carbon material with potential for electrochemical energy storage device applications due to its superb characteristics of chemical stability,<sup>27</sup> high electrical conductivity,<sup>28,29</sup> and large surface area.<sup>29,30</sup> Recently, it has been proposed that graphene should be a competitive material for supercapacitor application,<sup>31</sup> and two graphene supercapacitor application studies have been reported with the specific capacitance of 117 F/g in aqueous H<sub>2</sub>SO<sub>4</sub><sup>32</sup> and 135 F/g in aqueous electrolyte<sup>4</sup> based on a multilayered graphene material. In contrast to the conventional high surface materials, the effective surface area of graphene materials as capacitor electrode materials does not depend on the distribution of pores at solid state,<sup>4</sup> which is different from the current supercapacitors fabricated with activated carbons and carbon nanotube.<sup>8,14,25,33</sup> Obviously, the effective surface area of graphene materials should depend highly on the layers, that is, single or few layered graphene with less agglomeration should be expected to exhibit higher effective surface area and thus better supercapacitor performance. Thus, in this work, we have used a gas–solid reduction process to prepare the graphene materials (GMs), and fabricated supercapacitor devices using these GMs as electrode materials and investigated their performance. The single-layered graphene oxide sheets were reduced using gas-based hydrazine reduction at room temperature. The reduced graphene materials produced by this method have a lower degree of agglomeration than the chemically modified graphene (CMG) prepared in aqueous solution at the high temperature.<sup>4</sup> We have obtained a maximum specific capacitance of 205 F/g at 1.0 V in aqueous electrolyte with energy density of 28.5 Wh/kg, which are the best results for graphene materials so far and also significantly higher than those of CNT-based supercapacitors.<sup>4,21,34</sup> Furthermore, the power density of the capacitors reaches as high as 10 kW/kg, higher than that for CNT-based supercapacitors.<sup>21</sup>

\* E-mail: yschen99@nankai.edu.cn.

<sup>†</sup> Nankai University.

<sup>‡</sup> Tianjin University.

## 2. Experimental Section

**2.1. Raw Materials.** Graphene oxide (GO) was synthesized by the modification of Hummers's method and described elsewhere.<sup>28,35</sup> Graphene oxide (100 mg) was placed in a Petri dish set in a vacuum desiccator, where a piece of filter paper saturated with the chemical reducing agent hydrazine (80 wt % water solution, 5 mL) was placed in the desiccator for the reduction. The reducing reaction time of 72 h gave the best results for the capacitor performance as discussed below and this sample was assigned as GM-A. Two other graphene samples have also been prepared: sample GM-B, reduced in 24 h by hydrazine, and sample GM-C, obtained from GM-B after being further annealed at 400 °C for 3 h in argon.

**2.2. Fabrication of Supercapacitor Electrodes.** The supercapacitor test cells were fabricated with the two-electrode configuration. The electrodes were made of GMs, mixed with 10 wt % polytetrafluoroethylene (PTFE) binder electrodes. The two GM electrodes were separated by a thin polypropylene film in 30 wt % KOH aqueous electrolyte solution. The mixture of GMs and PTEF was homogenized in water by being sonicated for 30 min, and then dried for 18 h at vacuum oven at 120 °C to make water completely evaporate. The electrodes, which were pressed on a Ni foam current electrode ( $\Phi = 13$  mm) with a pressure of 20 MPa, were separated by a polypropylene film and were sandwiched in a stainless steel (SS) cell with a pressure of 160 MPa.

**2.3. Electrochemical Measurements.** The electrochemical properties and capacitance measurements of supercapacitor electrodes were studied in a two-electrode system by cyclic voltammetry (CV) and electrochemical impedance spectroscopy (EIS) using a Princeton Applied Research PARSTAT 2732 instrument, and galvanostatic charge–discharge was carried out with a supercapacitor tester (Arbin Instrument, USA). The cyclic voltammetry (CV) response of the electrodes were measured at different scan rates varying from 1 mV/s to 100 mV/s. Voltammetry testing was carried out at potentials between 0 and 1.0 V using a 30 wt % KOH aqueous electrolyte solution. Impedance spectroscopy measurements were carried out at a dc bias of 0.1 V with sinusoidal signal of 5 mV over the frequency range from 100 kHz to 1 mHz.

**2.4. Characterization.** Typical tapping-mode atomic force microscopy (AFM) measurements were performed using Multimode SPM from Digital Instruments with a Nanoscope IIIa Controller. Graphene oxide for AFM images were prepared by spin-coating the dispersion of graphene oxide in water (1.0 mg/mL) onto a freshly cleaved mica surface (500 rpm, 12 s; 2000 rpm, 30 s) and allowing them to dry in air. Scanning electron microscopy (SEM) was performed on LEO 1530 VP field emission scanning electron microscope with acceleration voltage of 10 kV. The electrical conductivity of GMs film was measured using the standard four-point contact method. Data were collected with a Keithley SCS 4200. The aqueous solution of graphene oxide (10 mg/mL) was spin-coated onto a glass slide (500 rpm, 12 s; 1000 rpm, 30 s), and subsequently the film was carried out with the hydrazine reduction strictly according to the same procedures for the preparation of GMs. Au electrodes were then vacuum deposited on the film and then the conductivity was measured using a standard four-probe method. N<sub>2</sub> adsorption–desorption analysis was done at 77 K on a Micromeritics ASAP 2020 apparatus. Elemental analysis was performed on Yanaca CDRDER MT-3 instrument.

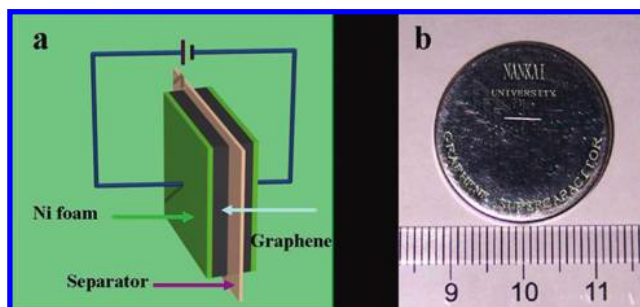


**Figure 1.** Graphene-based supercapacitor device. (a) Schematic diagram of graphene-based supercapacitor device. (b) An optical image of an industry-grade coin-shaped graphene-based supercapacitor device assembled in this study.

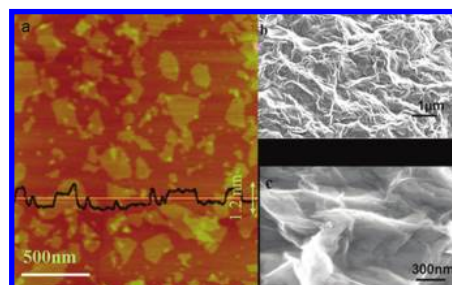


**Figure 2.** Morphology of graphene oxide and GMs. (a) Tapping-mode AFM image of graphene oxide and height profile plot showing the  $\sim 1.2$  nm thickness for individual graphene oxide sheets. The sample was prepared by spin-coating the dilute graphene oxide dispersion (1.0 mg/mL) onto a freshly cleaved mica surface. (b, c) Scanning electron microscopy (SEM) images of GM-A with different scale bars.

## 3. Results and Discussion

The supercapacitor devices are fabricated in the same way as in industry as shown in Figure 1. The procedure for the fabrication is detailed in the Experimental Section. The two-electrode capacitor configuration is used for these measurements because it provides the most reliable results of a material's performance for electrochemical capacitors.<sup>4</sup>

Figure 1a shows the schematic diagram of the graphene-based supercapacitor device, and it depicts the experimental arrangement used to assemble the supercapacitor devices. The thin film electrodes are fabricated by using the GMs with polytetrafluoroethylene (PTFE) as the binder. Figure 1b is an optical image of a real coin-shaped graphene-based supercapacitor device assembled in this study.

Supercapacitors are electrochemical capacitors that store the charge electrostatically using the reversible adsorption of ions of the electrolyte onto active materials that have high accessible specific surface area (SSA).<sup>5,8</sup> Thus, the efficacious adsorption of electrolyte ions is one of the keys to generate high specific capacitance.<sup>9</sup> Graphene, provided existing in individual single-layered sheet, can be assumed to offer an ideal material that both of its molecular sides could expose to the electrolyte with possibly highest surface area, and thus it may result in high specific capacitance. GMs are prepared from graphene oxide using a modified Hummers method.<sup>28,35</sup> Tapping-mode atomic force microscope (AFM) images of graphene oxide in Figure 2a demonstrate that the graphene oxide sheets exist as one-layer carbon sheets.<sup>29,36</sup> Graphene oxide is soluble in water, but has relatively low conductivity due to the damage of the graphene network in the preparation process.<sup>36</sup> Thus it may not be a good choice to be used directly for the supercapacitor application. Different methods have been developed for the

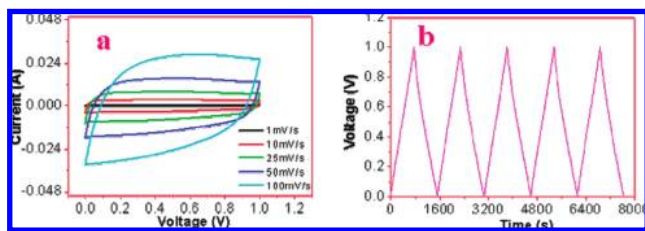


**Figure 3.** (a) Cyclic voltammograms (CV) for GM-A electrodes at different scan rates using 30 wt % KOH aqueous electrolyte. CV at high 100 mV/s still shows a rectangular-like curve, indicating a good capacitor behavior. (b) Galvanostatic charge–discharge curve of GMs electrode at a constant current density of 100 mA/g, using 30 wt % KOH electrolyte.

restoration of the graphene network, but direct annealing or solution reduction could cause significant agglomeration of the graphene sheets if no other force exists to prevent such agglomeration, as observed in many cases.<sup>4,35–37</sup> Hence, we use a gas-based hydrazine reduction to restore its graphene structure and conductivity, where the state of individual graphene oxide sheets is kept at maximum level for high effective and accessible surface area for electrolyte. This process should not lead to severe agglomeration of the graphene sheets as in other methods.<sup>37</sup> Field-emission scanning-electron microscopy (SEM) images of GM-A with different scale bars are shown in Figure 2b and Figure 2c. While the graphene sheets still exist as aggregated and crumpled sheets closely associated with each other, and form a continuum conducting network, these SEM images indeed suggest GM-A has a low degree of agglomeration compared with the graphene material in the earlier work with a solution reduction process.<sup>4</sup> In this structure or morphology the electrolyte ion should have better accessibility, not only penetrated in the outer region of the solids but also the inner region compared with the conventional carbon materials used in capacitors. So both sides of a broad range of graphene sheets could be exposed to the electrolyte and thus contribute to the capacitance. The C/N and C/O atomic ratio of GM-A by elemental analysis is 15.1 and 7.3, respectively. It has been reported that the heteroatoms and functional groups on the carbon sheets may improve the wettability of electrode, due to the increased number of hydrophilic polar sites,<sup>23,38–40</sup> and thus enhance the overall capacitor performance.

The performance of the supercapacitor devices using GMs is analyzed using cyclic voltammetry (CV), galvanostatic charge/discharge, and electrical impedance spectroscopy (EIS). The specific capacitance is calculated from the slope of the charge–discharge curves.<sup>33</sup> The EIS data is analyzed using Nyquist plots. Each data point in Nyquist plot is at a different frequency.<sup>33</sup>

Figure 3a shows cyclic voltammograms (CVs) of the graphene-based supercapacitor devices for sample GM-A with various scan rates in the range of 0 to 1 V. The presence of heteroatoms and functional groups in GM-A is supposed to contribute some pseudocapacitance,<sup>23,38</sup> however, the linear current with the increase of voltage indicates that there is little faradic in nature for our capacitors.<sup>4</sup> As we all know, the shape of the CV loop of a supercapacitor should be rectangular provided that there are low contact resistances,<sup>33</sup> and larger resistance distorts the loop, resulting in a narrower loop with an oblique angle.<sup>22,33</sup> The CVs of our devices are close to being rectangular with various scan rates (Figure 3a) and even at a high scan rate of 50 mV/s, indicating an excellent capacitance behavior and low contact resistance in the capacitors.<sup>33</sup>

Galvanostatic cycling of supercapacitor electrodes is performed at a constant current density of 100 mA/g. As seen in Figure 3b,

the discharge curves are linear in the total range of potential with constant slopes, showing nearly perfect capacitive behavior.<sup>14,33,41,42</sup> The specific capacitance is evaluated from the slope of the charge–discharge curves, according to the equation  $C = I\Delta t / (m\Delta V)$ , where  $I$  is the applied current and  $m$  (7.4 mg, not including the mass of PEFE) is the mass of each electrode.<sup>14,33,41,42</sup> The maximum specific capacitance reaches  $\sim 205$  F/g, and the maximum storage energy can be calculated as 28.5 Wh/kg with  $CV_i^2/2$ ,<sup>24,33</sup> where  $C$  is the specific capacitance (205 F/g) and  $V_i$  is the initial voltage (1.0 V). The effective surface area of the GM-A as measured by the  $N_2$  absorption Brunauer–Emmett–Teller (BET) method is 320  $m^2/g$ . The specific capacitance per surface unit calculated<sup>33</sup> is 64  $\mu F cm^{-2}$ , much higher than 20  $\mu F cm^{-2}$  afforded by clean graphite,<sup>33</sup> which generally affords only one side of a graphene sheet to expose to electrolyte. We have noted that the experimental results for the specific surface area of graphene materials are generally much lower than the theoretical value ( $\sim 2600 m^2/g$ ) of graphene sheets,<sup>29,30</sup> and they also have relatively large variation for different samples and methods in the literature<sup>4,31,32</sup> and our results. Two possible reasons are (1) in many cases, complete removal of the physically absorbed solvents, water as in our cases, is difficult as we only tried the samples at 120 °C for better dispersion purpose in the matrix; and (2) the stacking variation of the 2-D graphene sheets caused with different samples and treatment can be very large. The value of specific capacitance 205 F/g is higher than those of CNT-based supercapacitors previously reported by Niu et al. (102 F/g)<sup>21</sup> and Lee et al. (180 F/g).<sup>13</sup> Our supercapacitor devices give higher specific capacitance, probably due to the high accessibility by electrolyte ion and effective use of the specific surface area and high electric conductivity ( $\sim 100$  S/m, see below). We have also obtained specific capacitance at different current density from 100 to 2000 mA/g, however, the results do not show much change.

Similar studies were carried out for the other two samples, and they gave lower specific capacitance of 90 F/g and 68 F/g, respectively. The reasons may lie in the following facts. First, sample GM-B was only reduced for 24 h and the restoration of the conjugated carbon is expected to be not as good as that of sample GM-A, which was reduced for 72 h.<sup>2,29</sup> Second, while the annealing process may further restore the graphene network, it may increase the aggregation of graphene sheets and remove the heteroatoms and functional groups. These should have a negative impact on the capacitor performance. Based on these results, further detailed studies were carried out for sample GM-A.

In Figure 4a, the Nyquist plot of supercapacitor with GM-A electrodes shows a straight line in the low-frequency region and an unobscured arc in the high frequency region. This high frequency loop (from  $\sim 73182$  Hz to  $\sim 76$  Hz) is related to the electronic resistance between the graphene nanosheet.<sup>43</sup> The inconspicuous arc in the high frequency region shows that the electronic resistance between the graphene nanosheet is low.<sup>33</sup> The slope of the 45° portion of the curve is called the Warburg resistance and is a result of the frequency dependence of ion diffusion in the electrolyte to the electrode interface.<sup>14,33,41,42</sup> As seen from Figure 4a and Figure 4b, the Warburg curve is shorter than other reported supercapacitor electrodes,<sup>33</sup> which is an indication that the GM-A has a short ion diffusion path. This shall facilitate the efficient access of electrolyte ions to the graphene surface. The vertical shape at lower frequencies indicates a pure capacitive behavior, representative of the ion diffusion in the structure of the electrode.<sup>44</sup> The more vertical the curve, the more closely the supercapacitor behaves as an ideal capacitor.<sup>4</sup> The magnitude of equivalent series resistance

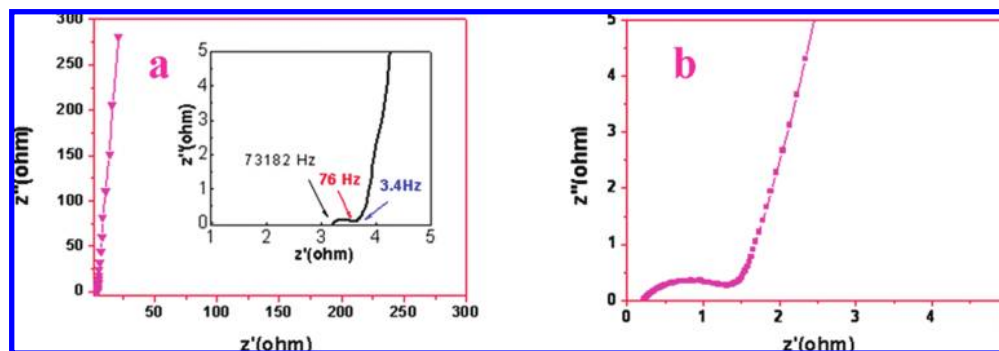


**Figure 4.** (a) Nyquist plots for GM-A electrodes with the stainless cell at a dc bias of 0.1 V with sinusoidal signal of 5 mV over the frequency range from 100 kHz and 1 mHz.  $Z'$ : real impedance.  $Z''$ : imaginary impedance. Inset shows an enlarged scale. (b) Nyquist plots for GM electrodes without the stainless cell at a dc bias of 0.1 V with sinusoidal signal of 5 mV over the frequency range from 100 kHz and 1 mHz.

(ESR) ( $3.2 \Omega$ ) is obtained from the  $x$ -intercept of the Nyquist plot in Figure 4a for GMs electrodes. ESR data determines the rate that the supercapacitor can be charged/discharged, and it is an important factor in determining the power density of a supercapacitor. To further study the electrical contact between the GM-A and together with the resistance between the GMs and the current collector, the EIS measurement of the supercapacitor without the SS cell is performed and its Nyquist plot is shown in Figure 4b. It is notable that the  $x$ -intercept of the Nyquist plot in Figure 4d was only 230 m $\Omega$ , much smaller than the ESR ( $3.2 \Omega$ ) with SS structure. This clearly indicates that the relatively large ESR value ( $3.2 \Omega$ ) with SS structure is due to the high resistance resulted by the stainless steel (SS) cell used to encapsulate the supercapacitor. Importantly, this additional measurement demonstrates that both the resistance of GMs and the contact resistance between the GMs and current collector Ni foam are low.

The maximum power density of the supercapacitor has been calculated from the low frequency data of the impedance spectra,<sup>14,33</sup> according to the equation  $P_{\max} = V_i^2/4mR$ ,<sup>33</sup> where  $V_i$  is the initial voltage,  $R$  is the ESR and  $m$  is the mass of the two electrodes with a cell voltage of 1.0 V, an ESR of  $3.2 \Omega$  and a mass of  $8.2 \times 10^{-3}$  g (including the mass of PTFE). A maximum power density of  $\sim 10$  kW/kg was thus obtained. The high value of the power density is well suited for surge-power delivery applications.<sup>34,41</sup> Obviously, since the intrinsic resistance for our graphene-based supercapacitor is low and the SS structure has a large contribution to the overall ESR, the power density can be increased if the SS cell resistance is reduced. This work is currently underway.

Long cycle life of supercapacitor is important for its practical applications.<sup>5,33</sup> Figure 5 shows the variation of specific capacitance with cycle number for GM-A supercapacitor at a constant current density of 500 mA/g. Cycle lives in excess of 1200 cycles have been showed. As can be seen, the specific capacitance still remains at 170 F/g ( $\sim 90\%$ ) after 1200 cycles of testing. This illustrates that our graphene-based supercapacitor process good stability, lifetime and a very high degree of reversibility in the repetitive charge–discharge cycling.

#### 4. Conclusions

In summary, we have fabricated supercapacitors using graphene materials (GMs) and found that the GMs prepared using the gas-based hydrazine reduction at room temperature gave remarkable results with specific capacitance of 205 F/g, energy density of 28.5 Wh/kg and power density of 10 kW/kg. The high value of the power density  $\sim 10$  kW/kg is well suited for surge-power delivery applications. While further detailed

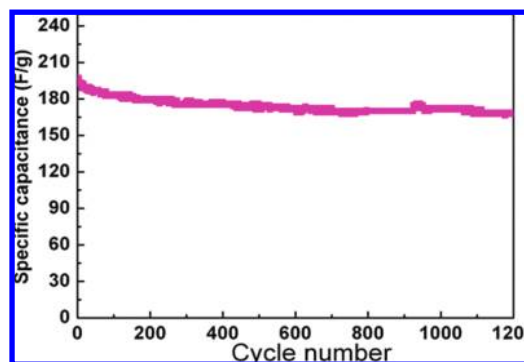


**Figure 5.** The specific capacitance change at a constant current density of 500 mA/g as a function of cycle number.

studies and optimization are needed, we strongly believe that graphene-based materials will lead to the development of high performance supercapacitors.

**Acknowledgment.** The authors gratefully acknowledge the financial support from NSFC (#20774047), MOST (#2006CB932702), MOE (#708020) of China and NSF of Tianjin City (#07JCYBJC03000 and #08JCZDJC25300).

#### References and Notes

- (1) Arico, A. S.; Bruce, P.; Scrosati, B.; Tarascon, J. M.; Van, S. W. *Nat. Mater.* **2005**, *4*, 366.
- (2) Pandolfo, A. G.; Hollenkamp, A. F. *J. Power Sources* **2006**, *157*, 11.
- (3) Winter, M.; Brodd, R. J. *Chem. Rev.* **2004**, *104*, 4245.
- (4) Meryl, S. D.; Sungjin, P.; Yanwu, Z.; Jinho, A.; Rodney, R. S. *Nano Lett.* **2008**, *8*, 3498.
- (5) Simon, P.; Gogotsi, Y. *Nat. Mater.* **2008**, *7*, 845.
- (6) Kotz, R.; Carlen, M. *Electrochim. Acta* **2000**, *45*, 2483.
- (7) Miller, J. R.; Simon, P. *Science* **2008**, *321*, 651.
- (8) Diederich, L.; Barborini, E.; Piseri, P.; Podesta, A.; Milani, P. *Appl. Phys. Lett.* **1999**, *75*, 2662.
- (9) Futaba, D. N.; Hata, K.; Yamada, T.; Hiraoka, T.; Hayamizu, Y.; Kakudate, Y.; Tanaike, O.; Hatori, H.; Yumura, M.; Iijima, S. *Nat. Mater.* **2006**, *5*, 987.
- (10) Lipka, S. *IEEE Aerosp. Electron. Syst. Mag.* **1997**, *12*, 27.
- (11) Lota, G.; Centeno, T. A.; Frackowiak, E.; Stoeckli, F. *Electrochim. Acta* **2008**, *53*, 2210.
- (12) Talapatra, S.; Kar, S.; Pal, S. K.; Vajtai, R.; Ci, L.; Victor, P.; Shaijumon, M. M.; Kaur, S.; Nalamasu, O.; Ajayan, P. M. *Nat. Nanotechnol.* **2006**, *1*, 112.
- (13) An, K. H.; Kim, W. S.; Park, Y. S.; Moon, J.-M.; Bae, D. J.; Lim, S. C.; Lee, Y. S.; Lee, Y. H. *Adv. Funct. Mater.* **2001**, *11*, 387.
- (14) Qu, D. Y. *J. Power Sources* **2002**, *109*, 403.
- (15) Shaijumon, M. M.; Ou, F. S.; Ci, L. J.; Ajayan, P. M. *Chem. Commun.* **2008**, 2373.
- (16) Toupin, M.; Brousse, T.; Belanger, D. *Chem. Mater.* **2004**, *16*, 3184.
- (17) Sugimoto, W.; Iwata, H.; Yasunaga, Y.; Murakami, Y.; Takasu, Y. *Angew. Chem., Int. Ed.* **2003**, *42*, 4092.

- (18) Miller, J.; Dunn, B.; Tran, T.; Pekala, R. *J. Electrochem. Soc.* **1997**, *144*, L309.
- (19) Rudge, A.; Davey, J.; Raistrick, I.; Gottesfeld, S.; Ferraris, J. *J. Power Sources* **1994**, *47*, 89.
- (20) Liu, C. G.; Liu, M.; Li, F.; Cheng, H. M. *Appl. Phys. Lett.* **2008**, *92*, 143108.
- (21) Niu, C. M.; Sichel, E.; Hoch, R.; Moy, D.; Tennent, H. *Appl. Phys. Lett.* **1997**, *70*, 1480.
- (22) Yoon, B. J.; Jeong, S. H.; Lee, K. H.; Kim, H. S.; Park, C. G.; Han, J. H. *Chem. Phys. Lett.* **2004**, *388*, 170.
- (23) Hulicova, D.; Yamashita, J.; Soneda, Y.; Hatori, H.; Kodama, M. *Chem. Mater.* **2005**, *17*, 1241.
- (24) Raymundo-Pinero, E.; Leroux, F.; Beguin, F. *Adv. Mater.* **2006**, *18*, 1877.
- (25) Yang, C. M.; Kim, Y. J.; Endo, M.; Kanoh, H.; Yudasaka, M.; Iijima, S.; Kaneko, K. *J. Am. Chem. Soc.* **2007**, *129*, 20.
- (26) Novoselov, K. S.; Geim, A. K.; Morozov, S. V.; Jiang, D.; Zhang, Y.; Dubonos, S. V.; Grigorieva, I. V.; Firsov, A. A. *Science* **2004**, *306*, 666.
- (27) Geim, A. K.; Novoselov, K. S. *Nat. Mater.* **2007**, *6*, 183.
- (28) Becerril, H. A.; Mao, J.; Liu, Z. F.; Stoltenberg, R. M.; Bao, Z.; Chen, Y. S. *ACS Nano* **2008**, *2*, 463.
- (29) Stankovich, S.; Dikin, D. A.; Piner, R. D.; Kohlhaas, K. A.; Kleinhammes, A.; Jia, Y.; Wu, Y.; Nguyen, S. T.; Ruoff, R. S. *Carbon* **2007**, *45*, 1558.
- (30) Stankovich, S.; Dikin, D. A.; Dommett, G. H. B.; Kohlhaas, K. M.; Zimney, E. J.; Stach, E. A.; Piner, R. D.; Nguyen, S. T.; Ruoff, R. S. *Nature* **2006**, *442*, 282.
- (31) Yongchao, S.; Edward, T. S. *Chem. Mater.* **2008**, *20*, 6792.
- (32) Vivekchand, S. R. C.; Rout, C. S.; Subrahmanyam, K. S.; Govindaraj, A.; Rao, C. N. R. *J. Chem. Sci.* **2008**, *120*, 9.
- (33) Conway, B. E. Kluwer Academic/Plenum Publishers: New York, 1999; Chapter 15.
- (34) Du, C. S.; Yeh, J.; Pan, N. *Nanotechnology* **2005**, *16*, 350.
- (35) Hummers, W. S.; Offeman, R. E. *J. Am. Chem. Soc.* **1958**, *80*, 1339.
- (36) Schniepp, H. C.; Li, J. L.; McAllister, M. J.; Sai, H.; Herrera, A. M.; Adamson, D. H.; Prud-homme, R. K.; Car, R.; Saville, D. A.; Aksay, I. A. *J. Phys. Chem. B* **2006**, *110*, 8535.
- (37) Gilje, S.; Han, S.; Wang, M.; Wang, K. L.; Kaner, R. B. *Nano Lett.* **2007**, *7*, 3394.
- (38) Hulicova, D.; Kodama, M.; Hatori, H. *Chem. Mater.* **2006**, *18*, 2318.
- (39) Lota, G.; Grzyb, B.; Machnikowska, H.; Machnikowski, J.; Frackowiak, E. *Chem. Phys. Lett.* **2005**, *404*, 53.
- (40) Lota, G.; Lota, K.; Frackowiak, E. *Electrochem. Commun.* **2007**, *9*, 1828.
- (41) Burke, A. *J. Power Sources* **2000**, *91*, 37.
- (42) Nishino, A. *J. Power Sources* **1996**, *60*, 137.
- (43) Portet, C.; Taberna, P. L.; Simon, P.; Laberty-Robert, C. *Electrochim. Acta* **2004**, *49*, 905.
- (44) Chen, W. C.; Wen, T. C.; Teng, H. S. *Electrochim. Acta* **2003**, *48*, 641.

JP902214F